SF2A 2007
J. Bouvier, A. Chalabaev, C. Charbonnel (eds)

HI IN CIRCUMSTELLAR ENVELOPES AROUND AGB STARS: OBSERVATIONS AND MODELLING OF THE DETACHED SHELL AROUND THE CARBON STAR Y CVN.

Y. Libert[1], T. Le Bertre[1] and E. Gérard[2]

Abstract. The history of the mass loss experienced by stars on the Asymptotic Giant Branch (AGB) is a key issue for describing the late stages of evolution of low and intermediate mass (1 - 6 $M_{\odot}$) stars, as well as an important ingredient for the characterization of the cosmic cycle of matter. As the mass-loss rates of AGB stars are variable, it is difficult to establish a balance of the mass loss over the long periods of time that need to be considered (10^4 - 10^6 years). As hydrogen is the main constituent of the stellar wind, the HI line at 21 cm should be a useful tracer of circumstellar environments (CSEs) for stars with an effective temperature larger than 2500 K, in which case the hydrogen in the envelope is mostly atomic. Therefore HI emission could be a diagnostic probe of the late stages of stellar evolution. Y CVn is such an example and shows the strongest HI line to date. We can detect both the HI counterpart of the CO emission coming from the inner envelope and the HI counterpart of the IR emission in the outer envelope. The HI profile is composed of two features: a narrow ($\sim$ 3 km.s^{-1}) and strong one ($\sim$400 mJy) that we associate with the latter and a faint ($\sim$10 mJy), broad ($\sim$ 15 km.s^{-1}), rectangular one that we associate with the former. The high spectral resolution that can be obtained at λ = 21 cm allows to constrain the physical conditions in the CSEs.

1 Introduction

During the Asymptotic Giant Branch (AGB) phase, the star surrounds itself with a shell made of dust and gas. The production of dust leads to an increase of the mass-loss rate: the dust accelerated by the radiation pressure drags away the gas. This mass-loss process can be so important that it controls the evolution of the star. The circumstellar gas flows into the interstellar medium (ISM) which is thus enriched with C, O, He and other heavier elements such as s-elements formed by neutron capture. Since the typical time on the AGB is around 10^5 - 10^7 years, a wind expanding at $V_{exp} \sim$ 10 km.s^{-1} can extend far from the star (0.5-1 pc). Determining the mass-loss rates of red giants is generally based on modelling radio molecular line profiles or infrared continuum energy distributions. Many rotational lines have been detected in circumstellar envelopes (e.g.: Knapp et al. 1998) and allow to explore a region limited to the inner part of the circumstellar shell, due to the photodissociation (0.01-0.1 pc) of molecules by the interstellar radiation field (ISRF). Many AGB stars were also detected with a far-IR excess by IRAS at 60 and 100 μm (Young et al. 1993) and later by ISO and the Spitzer Space Telescope. These observations put constraints on the shell thickness as well as on the mass-loss rate but cannot provide the spectral information needed to describe the kinematics.

The ideal tracers are obviously H_2 and HI which make up most of the CSE mass. But H_2 is very difficult to observe and is affected by photodissociation. HI should be a better tracer because it is not photoionized by the ISRF. Atomic hydrogen is present down to the stellar surface if the effective temperature of the stellar atmosphere is above $\sim$ 2500 K (Glassgold & Huggins 1983). At lower temperatures, the hydrogen is mostly molecular and HI is produced indirectly by photodissociation of H_2 within the CSE; thus it will be weaker and its space and velocity distributions different from those of matter outflowing from the stellar atmosphere.

But HI line has its own drawbacks: the signal is weak and must be discriminated against the ubiquitous background HI gas. In order to get a minimum confusion, two conditions are required: first, the star should

[1] Observatoire de Paris, LERMA, CNRS UMR 8112, 75014 Paris, France
[2] Observatoire de Paris, GEPI, CNRS UMR 8111, 92195 Meudon, France

be far enough from the Galactic Plane. Second, its radial velocity with respect to the Local Standard of Rest (LSR) should be large.

The first detection of HI emission from an AGB star was made by Bowers & Knapp (1988) with the VLA, around o Ceti. Since 2001, using the upgraded Nançay Radiotelescope (NRT), we have detected about 50 AGB stars in emission, in particular RS Cnc (Gérard & Le Bertre 2003), EP Aqr & Y CVn (Le Bertre & Gérard 2004), and X Her (Gardan et al. 2006). Sometimes the HI profiles for these sources exhibit a composite spectrum with a narrow and a broad feature. In some cases, both components are centered at the same velocity (Y CVn, RS Cnc) whereas in other cases the narrow component is shifted with respect to the central star velocity (X Her, EP Aqr). In general, HI line profiles have a quasi-gaussian shape with a width smaller than observed in the CO lines which implies a slowing down in the external layers of the CSEs (Gérard & Le Bertre 2006).

Recently, Matthews & Reid (2007) used the Very Large Array in its most compact configuration (D) to investigate the environment of 5 AGB stars : RS Cnc, IRC+10216, EP Aqr, R Cas and R Aqr. Only RS Cnc is unambiguously detected with an HI emission coinciding with the star in both position and velocity. Its map shows a compact ($\sim 82''$) central emission and a tail extending $6'$ to the northwest most likely related to the object. For three other sources (IRC+10216, EP Aqr and R Cas) they detect a signal with a radial velocity consistent with the velocity of the star but spatially offset. R Aqr was not detected.

2 Model of an AGB detached shell

During the AGB phase, the stellar gas expands and interacts with the external medium, either the ISM or older envelopes. The wind is slowed down and sweeps up the external matter (e.g. Lamers & Cassinelli 1999, Chap. 12). The envelope around the central star results from the free expansion of the wind out to a shock materialized by the inner boundary of the detached shell (termination shock). This model is represented in Fig. 1: r_1 defines the termination-shock radius, r_f defines the interface between compressed material of stellar (CS) and interstellar (EX) origins and r_2 defines the external boundary (bow shock) at which the external medium is compressed by the expanding shell. In this case, the broad component can be produced by a free expanding wind at a constant velocity (which spatially corresponds to the inner part of the shell). We assume an adiabatic shock inside r_1 which produces a drop of about a factor of 4 in velocity (e.g. Dyson & Williams 1997). This also constrains the density and the temperature profiles. At the shock in r_1, the temperature increases and, away from the shock region, the gas is expected to cool down out to r_f. The compressed external material should also experience an increase of temperature in r_2 and then a cooling down from r_2 to r_f.

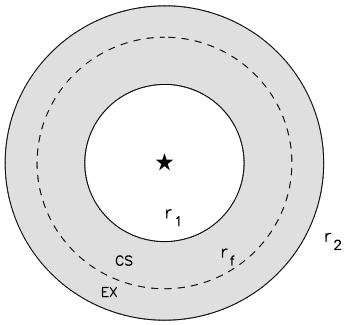

Fig. 1. Schematic view of a detached shell

The numerical code consists in a resolution of the one-dimensional eulerian equations using a classical Runge-Kutta method. The output is a set of 3 profiles of density, velocity and temperature as a function of radius. Once the profiles are computed, they are injected in another program which synthesizes the radiotelescope response (Gardan et al. 2006).

3 Y CVn and its circumstellar environment

Y CVn is a carbon star, 218 pc distant from the Sun (Hipparcos parallax : 4.59 ± 0.73 mas, Perryman et al. 1997). This corresponds to a distance of 207 pc above the Galactic Plane. The K magnitude is -0.74 (Guandalini et al. 2006) which translates to a bolometric magnitude of 1.96 (Le Bertre et al. 2001) or $\sim$ 6200 $L_\odot$ at 218 pc. Such a luminosity places the star clearly on the AGB, probably on the early AGB (E-AGB) rather than on the thermally pulsing AGB (TP-AGB). Indeed Y CVn is a J-type carbon star with a $^{12}CO/^{13}CO$ ratio of about 3.5 (Lambert et al. 1986). This suggests that it has not gone through thermal pulses, because J-type stars are not enriched in s-process elements. The effective temperature found by Bergeat et al. (2001) is T_{eff} = 2760 K.

The first evidence of a circumstellar shell around Y CVn was found by Goebel et al. (1980) who detected the emission band of SiC at 11.5 μm. The shell was then searched for CO rotational lines and Knapp et al. (1998) first detected the CO(3-2) emission with the CSO. They derived a LSR radial velocity of V_{LSR}=21.1 km.s^{-1}, an expansion velocity of V_{exp}=7.8 km.s^{-1} and a mass-loss rate of $\dot{M}$ = 1.1 10^{-7} $M_\odot$.yr^{-1}. Later, those results were confirmed by other transitions of CO (Schoïer et al. 2002, Teyssier et al. 2006). The emission has been found extended by $\sim$13″ ($\sim$ 0.014 pc) in the 1-0 line and $\sim$9″ in 2-1 (Neri et al. 1998).

An extended emission was also discovered by IRAS (Young et al. 1993) at 60 μm and 100 μm. The emission could be modelled with a resolved isothermal shell of inner radius r_{in} $\sim$ 2.8′ ($\sim$ 0.18 pc) and outer radius r_{out} $\sim$ 5.5′. This detection was confirmed by ISO at 90 μm (Izumiura et al. 1996) with a higher resolution ($\sim$ 40″). In the ISO image, r_{in} is $\sim$ 2.8′ and r_{out}, $\sim$ 5.1′ ($\sim$ 0.32 pc). The ISO image also showed a slight offset of about 1′ to the West.

We have selected this source to test the model presented in Sect. 2 because it is the brightest in our HI survey, and because its HI emission does not suffer from interstellar confusion. Also the ISO image has a nearly circular shape and we expect that the geometry does not differ too much from a spherical one. Finally, with an effective temperature larger than 2500 K, we expect that the hydrogen is mainly in atomic form (Glassgold & Huggins 1983), such that we need not take into account the photodissociation of molecular hydrogen.

4 Observations of Y CVn with the NRT

The NRT consists of a rectangular tiltable mirror (effective dimension 160x30m), a spherical mirror (300m long and 35m high) and a focal carriage on a curved rail track. This meridian instrument can follow a source for about 60 min. At 1420 MHz, its spatial resolution is 4′ in Right Ascension and 22′ in Declination. Since the FORT project (van Driel et al. 1996), the focal system has been entirely renovated resulting in a typical system temperature of 35K. Such a collecting area and sensitivity allow to efficiently detect weak extended sources. The data were acquired in the position-switch mode. This process efficiently removes the galactic background HI emission (in case of a non-quadratic spatial variation). A total of 107 hours was spent on Y CVn between Sept. 2002 and Jan. 2007. The spectra obtained have a final resolution of 0.32 km.s^{-1}.

The central spectrum is composed of two features (Fig. 3). The first component (Comp. 1) is narrow, quasi-gaussian shaped with a FWHM of $\sim$3.1 km.s^{-1}. The second (Comp. 2) is a rectangle of 10 mJy height and 15.6 km.s^{-1} width. Comp. 2 half width (7.8 km.s^{-1}) is consistent with the expansion velocity given by CO observations (see Sect. 3). No evidence of such a pedestal was found in the offset positions which tends to indicate that the region traced by Comp. 2 extends no further than $\sim$ 2′ radius.

The map (Fig. 2) shows a quasi-circular image. According to the difference between the peak intensities of the two East and West offset spectra and that of the central spectrum, we deduce a displacement of $\sim$1′ West which is consistent with the ISO image at 90 μm (see Sect. 3). This offset is small compared to the HI shell size that we can estimate from the map at 8′$\pm$4′. At this wavelength and with this low surface density, the HI emission is optically thin. Therefore, the total integrated flux received from the source is directly proportional to the HI mass. With a mean molecular weight of 1.3 (i.e. 10% He, 90% H) we deduce a total mass of the envelope of $\sim$ 4.9 10^{-2} $M_\odot$.

5 Interpretation and discussion

We applied the model described in Sect. 2 to Y CVn, setting r_1 $\sim$ 2.8′ and r_2 $\sim$ 5.1′ in agreement with the IR results (see Sect. 3). According to the HI observations, the region between the central star and r_1 is freely expanding at a velocity V_{exp} $\sim$ 7.8 km.s^{-1}. The total mass included in this region is thus given by the area of

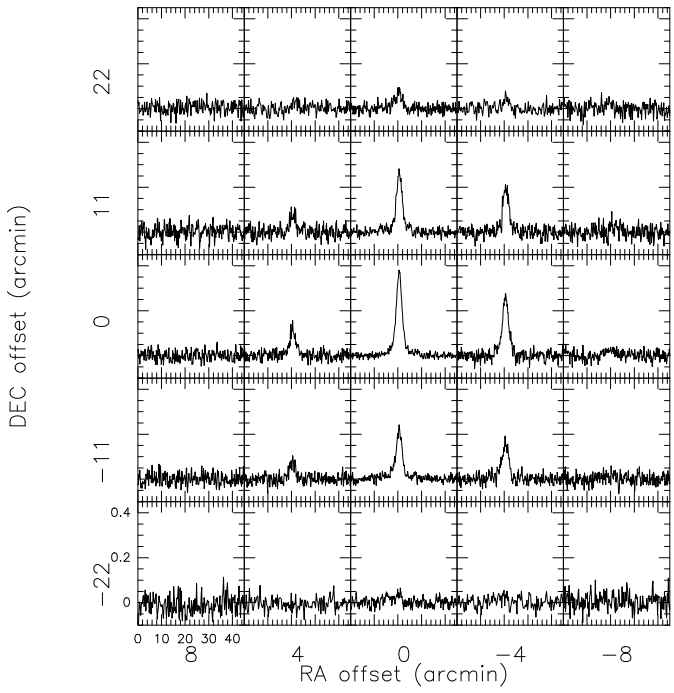

Fig. 2. Y CVn map obtained with the NRT. The step in RA is 4′ and 11′ in Dec.

	V_{cent} (km.s^{-1})	Width (km.s^{-1})	F_{peak} (mJy)
Comp. 1 (center)	20.5	3.1	358.
Comp. 2 (center)	21.1	15.6	10.
Comp. 1 (± 4′ in RA)	20.5	3.2	179.
Comp. 1 (± 11′ in Dec.)	20.6	3.1	232.
Comp. 1 (± 11′ in Dec. and ± 4′ in RA)	20.5	3.2	132.

Table 1. Results of a gaussian (Comp. 1) and a rectangular (Comp. 2) fit.

the pedestal: $M_p \sim 2.3\ 10^{-3}\ M_\odot$. To evaluate the mass-loss rate, we use: $\dot{M} = M_p.V_{exp}/r_1$ and find $\dot{M} \sim 1\ 10^{-7}\ M_\odot.yr^{-1}$, in remarkable agreement with the CO estimate.

At a given mass-loss rate, the code uses the mass conservation equation and distributes all the material throughout the shell (for more precisions see Libert et al. 2007). This gives a value of $r_f \sim 4.2'$ and a total age for the shell of $\sim 4\ 10^5$ years. For a maxwellian distribution of atoms at a given temperature, the emission projected on the line of sight has a gaussian shape with a width directly related to the mean temperature in the shell. It provides an upper limit to the mean temperature $T_{mean} \sim 210$ K. As explained in Sect. 2, the gas is heated by the shock and we estimate the temperature behind r_1 at ~ 1800 K. Therefore from r_1 to r_f the gas must cool from ~ 1800 K to less than 200 K in $\sim 4\ 10^5$ years. We choose not to estimate the cooling rate in the shell which should depend on the emission lines of carbon or oxygen and therefore on metallicity. We rather adopt an empirical law:

$$log\frac{T}{T_1} = a\ log\frac{r}{r_1} \tag{5.1}$$

with T_1 the temperature behind the shock and a the only free input parameter in this computation. It allows to change the gradient of the temperature within the shell.

The results of our model (Fig. 3) are in good agreement with the observations. We notice a slight shift of ~ 1 km.s^{-1} between the observed Comp. 2 and the model (right panel in Fig. 3). This is probably related to the asymmetry found in the map of Y CVn (see Sect. 4). Indeed, in the model, we assume spherical symmetry and

do not take into account the motion of the star with respect to its surrounding external matter. This motion should cause a stronger slowing down in the direction of motion. This is consistent with the proper motion obtained by Hipparcos: the source is moving at 13.4 mas.yr^{-1} in RA and 17.4 mas.yr^{-1} in Dec. (corrected for solar motion) which corresponds to a motion in the plane of the sky towards the North-East.

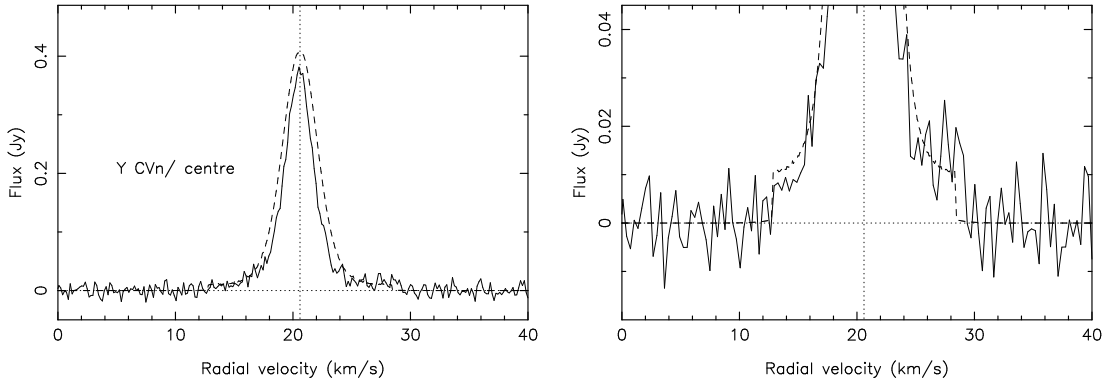

Fig. 3. HI spectrum obtained on the star position with the NRT (full line) and model (dashed line). The right panel is a zoom to enhance the pedestal (Comp. 2). The vertical dotted line indicates the central velocity adopted for the modelling.

Recently, evidences for the interaction between stellar wind and external matter have been found. Using the Multiband Imaging Spectrometer of the Spitzer Space Telescope, Ueta et al. (2006) found a bow shock around the AGB star, R Hya. Assuming that it was a result of the motion of the star in the local medium, at a relative velocity of $\sim$ 35 km.s^{-1}, they derived a temperature behind the shock of $\sim$ 35000 K.

New results from the ultraviolet satellite GALEX also show a bow shock with a cometary shape around Mira and a trailing emission (Martin et al. 2007). According to these authors, this emission corresponds to an excitation of the molecular hydrogen in the post-shock region by the hot electrons ejected from the shock region. This emission extends to the north over 2° which is in good agreement with the proper motion of Mira.

6 Conclusion and perspectives

We revisited the observations of the bright carbon star Y CVn. The greatly improved quality over the former map (Le Bertre and Gérard 2004), allowed us to derive some important characteristics of the shell. The narrowness of Comp. 1 is an indisputable proof of a slowing down in the outer layer of the envelope. With a simple eulerian code, we modelled the interaction between the stellar wind and the external matter assuming a constant mass-loss rate. The results show that, with a mass-loss rate of $\sim$ 1 10^{-7} M$_{\odot}$.yr^{-1} and an age of the shell of 4 10^5 years, we can reproduce the HI emission of the Y CVn envelope.

But Y CVn is only one among several AGB stars detected with the NRT which will be good candidates for further investigation of the mass-loss process. There is a great diversity of HI profiles among the objects detected by Gérard & Le Bertre (2006). This likely reflects differences in mass-loss rate, chemical composition, age, expansion velocity and surrounding ISM. Four other sources discovered by the NRT have been observed with the VLA this spring and we plan to combine the single-dish (NRT) with these interferometric measurements.

The model developed for Y CVn will be improved and applied to determine the physical parameters of several other sources. We stress the importance of a high spectral resolution to study AGB outflows, which, in addition to having a low velocity (around few km.s^{-1}), are further decelerated by the interaction with the surrounding medium. The high resolution HI profiles should help us to describe the diversity and complexity of AGB outflows.

7 Acknowledgments

We thank the PCMI and the ASA for financial support. The Nançay Radio Observatory is the Unité scientifique de Nançay of the Observatoire de Paris, associated as Unité de Service et de Recherche (USR) No. B704 to the French Centre National de la Recherche Scientifique (CNRS).

References

Bergeat J., Knapik A., Rutily B., 2001, A&A, 369, 178
Bowers P.F., Knapp G.R., 1988, ApJ, 332, 299
Dyson J.E., Williams D.A., 1997, "*The Physics of the Interstellar Medium*", 2^{nd} edition, Institute of Physics Publishing
Gardan E., Gérard E., Le Bertre T., 2006, MNRAS, 365, 245
Gérard E., Le Bertre T., 2003, A&A, 397, L17
Gérard E., Le Bertre T., 2006, AJ, 132, 2566
Glassgold A.E., Huggins P.J., 1983, MNRAS, 203, 517
Goebel J.H., et al., 1980, ApJ, 235, 104
Guandalini R., Busso M., Ciprini S., Silvestro G., Persi P., 2006, A&A, 445, 1069
Izumiura H., Hashimoto O., Kawara K., Yamamura I., Waters L.B.F.M., 1996, A&A, 315, L221
Knapp G.R., Young K., Lee E., Jorissen A., 1998, ApJS, 117, 209
Lambert D.L., Gustafsson B., Eriksson K., Hinkle K.H., 1986, ApJS, 62, 373
Lamers J.G.L.M., Cassinelli J.,1999, *Introduction to stellar winds*, Cambridge University Press
Le Bertre T., Gérard E., 2004, A&A, 419, 549
Le Bertre T., Matsuura M., Winters J.M., et al., 2001, A&A, 376, 997
Libert Y., Le Bertre T., Gérard E., 2007, MNRAS, 381, 1161
Martin D.C., Seibert M., Neill J.D., et al., 2007, Nature, 448, 780
Matthews L.D., Reid M.J., 2007, AJ, 133, 2291
Neri R., Kahane C., Lucas R., Bujarrabal V., Loup C., 1998, A&AS, 130, 1
Perryman M.A.C., Lindegren L., Kovalevsky J., et al., 1997, A&A, 323, L49
Schöier F.L., Ryde N., Olofsson H., 2002, A&A, 391, 577
Teyssier D., Hernandez R., Bujarrabal V., Yoshida H., Phillips T.G., 2006, A&A, 450, 167
Ueta T., Speck A.K., Stencel R.E., et al., 2006, ApJ, 648, L39
van Driel W., Pezzani J., Gérard E., 1996, Proc. "High-Sensitivity Radio Astronomy", Jackson D. (ed.), 229
Young K., Phillips T.G., Knapp G.R., 1993, ApJS, 86, 517